Journal of Power Sources 193 (2009) 495–500

Contents lists available at ScienceDirect

Journal of Power Sources

journal homepage: www.elsevier.com/locate/jpowsour

Controlled synthesis of mesoporous carbon modified by tungsten carbides as an improved electrocatalyst support for the oxygen reduction reaction

Qing Zhu[a], Shenghu Zhou[b,c], Xiqing Wang[a], Sheng Dai[a,b,*]

[a] Chemical Sciences Division, Oak Ridge National Laboratory, Oak Ridge, TN 37831, USA
[b] Center for Nanophase Materials Sciences, Oak Ridge National Laboratory, Oak Ridge, TN 37831, USA
[c] Division of Fuel Cell and Energy Technology, Ningbo Institute of Material Technology and Engineering, Chinese Academy of Sciences, Ningbo 315201, China

ARTICLE INFO

Article history:
Received 10 February 2009
Received in revised form 15 April 2009
Accepted 16 April 2009
Available online 23 April 2009

Keywords:
Fuel Cell
Electrocatalysis
Mesoporous carbon

ABSTRACT

Mesoporous carbon was modified with tungsten carbides by the carbothermal hydrogen reduction of a layer of chemisorbed 1:12 phosphotungstic anions ($PW_{12}O_{40}^{3-}$) on carbon surfaces. Depending on the temperature of carbothermal treatment, different tungsten species, i.e., W, W_2C, WC, were formed on the carbon matrix. No significant changes in both surface areas and mesostructures were observed during the formation of various tungsten species on carbon surfaces under high-temperature conditions. A uniform dispersion of Pt nanoparticles (1–6 nm) can be achieved via nanoconfinement on the surfaces of both mesoporous carbon and tungsten carbide-modified mesoporous carbon. Pt nanoparticles supported on mesoporous carbons modified with tungsten carbide (Pt/WC-C) exhibit enhanced electrocatalytic activities relative to the control, in which mesoporous carbons without carbide modification were directly used as a support (Pt/C). In addition, both enhanced thermal stability and good electrochemical stability were observed for the Pt/WC-C electrocatalyst.

Published by Elsevier B.V.

1. Introduction

Proton exchange membrane fuel cells (PEMFCs) have been considered as alternative energy conversion devices in transportation vehicles and in small-scale stationary power supplies. However, the slow kinetics of the oxygen reduction reaction (ORR) and the poor durabilities of carbon supports at cathodes limit their application [1–3]. ORR on cathodes is such a slow reaction that an overpotential from 0.3 to 0.4 V is required under reasonable current conditions [4]. The poor durabilities of carbon-supported Pt catalysts can lead not only to the gradual corrosion of cathodes by the Pt-catalyzed oxidation but also to the agglomeration of Pt nanoparticles [1]. Both corrosion and agglomeration can result in an unacceptable rate of performance loss [5,6]. To improve the performance of cathodes, alternative and durable supports must be developed. The tendency of agglomeration of Pt nanoparticles can be fundamentally attributed to the lack of strong metal–support interactions between Pt nanoparticles and carbon supports [7]. Two key synthesis strategies to improve the sintering resistance of cathode materials are: (1) the use of space confinement to anchor Pt nanoparticles and (2) the surface modification of supports to enhance metal–support interactions. Recent studies suggest that mesoporous carbon presents a unique opportunity in development of high-performance carbon supports for Pt electrocatalysts because of its superior properties, such as facile mass transport and high surface area [8]. Notably, Ryoo and his co-workers have utilized a mesoporous carbon derived from a hard-templating synthesis for supporting Pt electrocatalysts in direct methanol fuel cells [9]. A high electrocatalytic activity was observed for such a catalytic system. We have recently investigated the use of mesoporous carbons derived from soft-templating synthesis [10] for confining Pt nanoparticles for electrocatalysis. Our results indicate that graphitized mesoporous carbon exhibits a considerably enhanced thermal stability and corrosion resistance [11]. Herein we describe an alternative approach to the further improvement of cathode performances based on surface functionalization of mesoporous carbons by tungsten carbides.

Tungsten carbides are known to have platinum-like catalytic behaviors [12,13]. Accordingly, they have been investigated as a potential candidate for both cathode and anode electrocatalysts of PEMFCs. Recently, a number of studies have shown that tungsten carbides can not only function as an alternative electrocatalyst to noble metals [14] but also promote the electrochemical activities of Pt catalysts in alkaline solution [4,15]. Although tungsten carbides can be prepared by many methods, such as alkalide reduction [16] and microwave-promoted solid-state reactions [17,18], the carbothermal reduction method, in which carbon reacts with tungsten-containing species under reductive environments (flowing H_2) [19,20], is the most popular approach for the synthesis of tungsten carbides on carbon support. The key issue associated

* Corresponding author at: Chemical Sciences Division, Oak Ridge National Laboratory, Oak Ridge, TN 37831, USA.
E-mail address: dais@ornl.gov (S. Dai).

0378-7753/$ – see front matter. Published by Elsevier B.V.
doi:10.1016/j.jpowsour.2009.04.017

with this synthesis method is the difficulty in producing tungsten carbides with high surface areas because of temperature-induced sintering. In our current study, two strategies were utilized to disperse tungsten carbides on carbon materials. Firstly, nonvolatile tungsten-containing polyoxometallate species were used as carbide precursors. The uniform dispersion of the polyoxometallate precursors was achieved through their unique surface chemisorption on carbons. Secondly, mesoporous carbons derived from soft-templating synthesis were employed as a host for tungsten carbides. The corresponding large mesopores and high thermal stabilities proved to be ideal for immobilization of spherical polyoxometallate nanoparticles. The strong cohesive interface with carbon supports and space confinement with mesopores can lead to a high dispersion of tungsten carbides on carbon surfaces.

2. Experimental

2.1. Preparation

Mesoporous carbon (C-ORNL-1) was prepared following the method previously established by our group [21]. The tungsten-modified mesoporous carbon was prepared through carbothermal reactions by employing 1:12 phosphotungstic acid ($H_3PW_{12}O_{40}$) as a precursor for tungsten carbides. Briefly, mesoporous carbon (~100 mg) was added into an aqueous solution of $H_3PW_{12}O_{40}$ (~32.6 mg) under stirring and the mixture was kept stirring at room temperature overnight. The slurry was centrifuged and washed thoroughly by deionized water to remove excess $H_3PW_{12}O_{40}$ molecules. After being dried at 120 °C under vacuum overnight, the resultant material was then thermally reduced in a tubular furnace under H_2/Ar. By controlling time and temperature of H_2 thermal reduction treatment, different compositions of tungsten carbides were obtained. The sample was cooled in H_2/Ar and then ground to fine powder for use as an electrocatalyst support.

Platinum electrocatalysts supported on different carbons including unmodified and modified mesoporous carbons as well as the commercial carbon (Vulcan XC-72R) were prepared using a wet impregnation method. To be consistent with commercial electrocatalysts, the samples with Pt loadings of ~9 wt% were prepared. An acetone solution of chloroplatinic acid ($H_2PtCl_6{\cdot}6H_2O$) with calculated amount of Pt was mixed with a suspension of carbon supports in acetone under stirring. After stirring for 2 h, the slurry was air-dried at room temperature to evaporate most of solvents and continued to dry in an oven at 40 °C overnight. The sample obtained was then reduced at 300 °C for 3 h under H_2, yielding ~9 wt% Pt on carbon supports.

2.2. Characterization

N_2 sorption isotherms were recorded on a Micromeritics Tristar analyzer at −196 °C (77 K). Prior to measurement, the sample was purged with flowing N_2 at 150 °C for 3 h. The specific surface area was calculated using the BET method from the nitrogen adsorption data in the relative range (P/P_0) of 0.06–0.20. The external surface area and micropore volume were calculated by the α_s method, where nonporous acetylene carbon black was used as a reference (its BET surface area is 69.4 $m^2\,g^{-1}$). The pore size distribution (PSD) plots were derived from the adsorption branch of the isotherms based on the BJH model. Transmission electron microscopy (TEM) was used to measure the particle size of Pt and tungsten carbides. X-ray diffraction (XRD) patterns were recorded to determine the formation of tungsten carbides and estimate the particle size of Pt. The loading of tungsten was estimated by energy-dispersive X-ray spectroscopy (EDX, EDAX Inc.). Thermal stability of electrocatalysts and loading of Pt were investigated by thermal gravimetric analysis (TGA, TA Instruments).

2.3. Electrochemical measurements

Cyclic voltammetry and linear sweep voltammetry measurements were performed in a three-electrode system consisting of a working electrode, an auxiliary electrode and a reference electrode. A glassy carbon rotating disk electrode (RDE, Pine Instrument) was used as a working electrode for evaluation of the electrochemical activities of electrocatalysts. An Ag/AgCl electrode was chosen as a reference electrode and Pt wire was used as an auxiliary electrode. The electrocatalyst electrode was prepared by first placing catalyst suspension (1.0 mg ml^{-1}) onto the surface of the glassy carbon disk (5 mm), followed by drying at room temperature. After air-drying, the electrode was covered with Nafion (0.05 wt%) to protect the catalyst from falling from the electrode. The electrochemical experiments were performed in oxygen-saturated 0.05 M H_2SO_4 aqueous solution at room temperature. To investigate the electrochemical activity of catalysts, the linear sweep voltammograms were recorded between 0 and 1.0 V versus the standard hydrogen electrode (SHE) at a scan rate of 10 mV s^{-1} and the rotation rate of 1600 rpm. The electrochemical activity of the carbon and tungsten carbide-modified carbon supports were also recorded. Although tungsten carbides exhibited electrochemical activity in alkaline solution, no electrochemical activity was found for tungsten carbides in acidic solution in this study (data not included in the paper). To test the electrochemical stability of electrocatalysts, 1000 cyclic voltammetry (CV) cycles were carried out in oxygen-saturated 0.05 M H_2SO_4 solution at a scan rate of 5 mV s^{-1} from ~0 to 1.0 V versus SHE. The linear sweep voltammograms were recorded before and after 1000 CV cycles so that changes of potential and current could be clearly compared. For all the electrochemical experiments, current density (current per mg of Pt, A mg^{-1}) was used to compare the performance of different electrocatalysts because of the small variation of the Pt loadings for different catalyst samples.

3. Results and discussion

A polyoxometallate compound of tungsten ($H_3PW_{12}O_{40}$) was employed as a precursor to prepare tungsten carbides in our current study. This polyoxometalate compound has a Keggin-type structure and is known to undergo a strong surface adsorption on carbons, leading to the formation of finely dispersed species on carbon surfaces [22–24]. The strong chemisorption of this 1:12 phosphotungstic anion [$PW_{12}O_{40}{}^{3-}$] on carbon surfaces has previously been used to prepare surface-modified electrodes for electroanalysis and electrocatalysis [25,26]. Recently, Zhou et al. have loaded [$P_2Mo_{18}O_{62}{}^{6-}$] anions on a mesoporous carbon (CMK-3) derived from SBA-15 and used such modified sample to fabricate a carbon paste electrode [27]. In this case, the pore size of CMK-3 was only ~4.5 nm, and thus the modified CMK-3 exhibited a considerably reduced mesoporosity. The molecular size (~1.1 nm) of [$PW_{12}O_{40}{}^{3-}$] is considerably less than the pore diameter (7.3 nm) of C-ORNL-1. Accordingly, we expect that our mesoporous carbon is an ideal support for dispersion of this polyoxometallate anion through the strong surface adsorption.

Phosphotungstic anions were loaded onto the surfaces of C-ORNL-1 via surface adsorption. The resulting products were then filtered, washed with distilled water to remove any excess or unadsorbed species, and dried at 120 °C. Because the external surface area of C-ORNL-1 is very small (28.2 $m^2\,g^{-1}$ by the α_s method), most of phosphotungstic anions are believed to be located on the inner surface. Fig. 1 shows the BET N_2 adsorption isotherms of the carbon materials before and after the surface modification of phosphotungstic anions. Clear decreases in the amount of N_2 uptake and the corresponding mesopore diameter by about 0.5 nm were

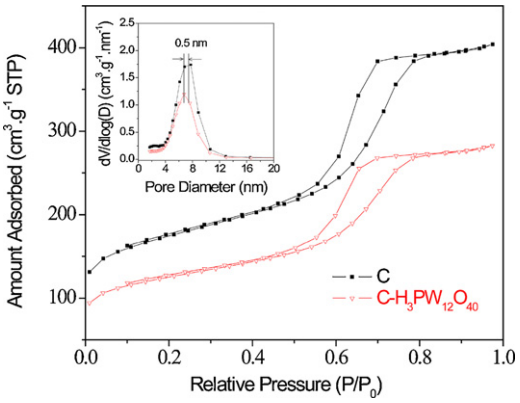

Fig. 1. N_2 sorption isotherms of C-ORNL-1 before and after modification with $H_3PW_{12}O_{40}$. The insert is the BJH pore size distribution plots.

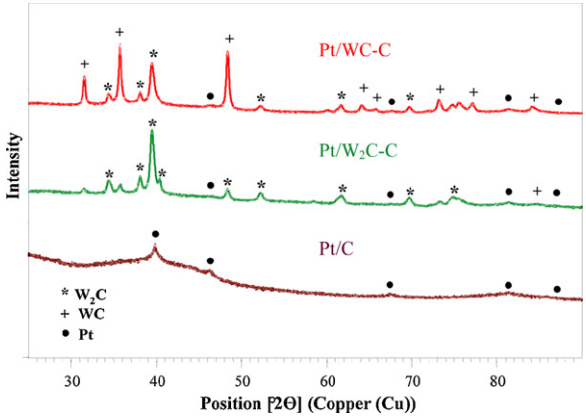

Fig. 3. XRD patterns of Pt/WC-C, Pt/W_2C-C, and Pt/C.

observed after surface modification, indicating the successful coverage of the mesopore surfaces by phosphotungstic anions. The tungsten content of the resulting material was estimated to be 16 wt% by EDX analysis. C-ORNL-1 exhibits a BET surface area of 610 $m^2\,g^{-1}$, of which about 270 $m^2\,g^{-1}$ arises from the contribution of mesopores. Since most of microporous surfaces might not be accessible to large [$PW_{12}O_{40}^{3-}$] anions, we assume the majority of [$PW_{12}O_{40}^{3-}$] anions are adsorbed on mesopore surfaces. If a monolayer of [$PW_{12}O_{40}^{3-}$] anions is formed on mesopore surfaces, the theoretical tungsten content should be close to 20 wt% based on a close packing of the polyoxoanions with a diameter of ~1.1 nm. Therefore, we believe that about 80% of carbon surfaces originating from mesopores are covered with [$PW_{12}O_{40}^{3-}$] anions.

The H_2 thermal reduction treatment of the [$PW_{12}O_{40}^{3-}$]-coated carbons at high temperature under H_2–Ar atmosphere was used to generate the corresponding tungsten carbides dispersed on our mesoporous carbons. It was found that the formation of tungsten species on mesoporous carbon was strongly dependent on calcination temperature. As shown in Fig. 2, a pure tungsten phase was generated initially at 600 °C, followed by the formation of a W_2C-dominated phase at 800 °C. Since W_2C is thermally unstable, the further increase of both calcination time and calcination temperature favors the conversion of W_2C to WC, resulting in a WC-dominated phase at 1200 °C. The tungsten species-modified mesoporous carbons were denoted as W-C, W_2C-C, and WC-C, respectively. Upon the formation of tungsten species after H_2 thermal reduction treatment, both specific surface areas and pore volumes decreased. However, little changes on pore size distributions were observed (Table 1). The results suggest that the basic structure of C-ORNL-1 was maintained during the formation of tungsten carbide species. This observation is in sharp contrast with

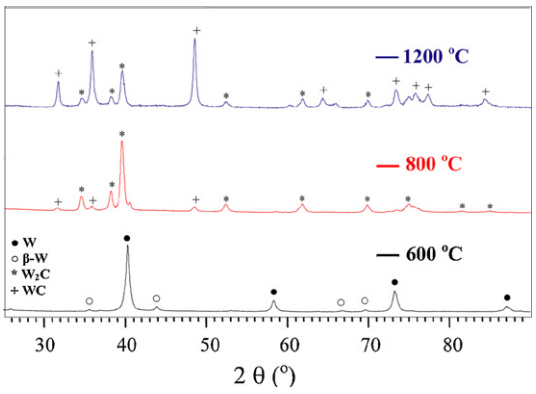

Fig. 2. XRD patterns of tungsten species formed at different temperatures.

the carbothermal reactions conducted with mesoporous carbon derived from hard-template synthesis. The mesopores of the latter system are connected through ultrathin carbon filaments, which are not stable under high-temperature conditions (>900 °C). The maintenance of the mesostructures is important to facilitate not only the anchor of Pt particles but also the mass transport of ORR. Accordingly, the electrocatalysts of Pt loaded on C-ORNL-1 and tungsten carbide-modified carbons were denoted as Pt/C, Pt/W_2C-C, and Pt/WC-C, respectively.

TEM were used to probe the average sizes of Pt nanoparticles formed on both surface-modified and unmodified mesoporous carbons. As seen from the XRD patterns, Pt nanoparticles can be readily introduced via incipient wetness on the surfaces of different carbon supports. The broad XRD diffraction peaks associated with Pt also suggested that the particle size of Pt on those carbon supports was small (Fig. 3). TEM results indicated that Pt nanoparticles with an average particle size of 2 nm were obtained on mesoporous carbon (Fig. 4B and C), consistent with XRD results. In contrast to Pt, WC nanoparticles were much larger (average particle size 10 nm) and dispersed on carbon surfaces (Fig. 4A). The actual Pt loadings for all catalysts, determined by TGA, were 9.6 wt% for Pt/C, 9.1 wt% for Pt/WC-C, 8.9 wt% for Pt/W_2C-C, and 8.5 wt% for Pt/XC-72R, respectively. The similarities in Pt loadings and Pt particle sizes suggested that the synergistic effect of tungsten carbide plays an important role in the enhancement of electrocatalytic activity of Pt/WC-C relative to Pt/W_2C and Pt/C. The TEM image also indicated that deposition of Pt on mesoporous carbon or tungsten carbide-modified mesoporous carbon was more uniform than that on XC-72R, suggesting an enhanced interaction between Pt and mesoporous carbon supports.

The electrochemical activities of our electrocatalysts were investigated using an RDE in acidic solution at room temperature. As shown in Fig. 5, Pt electrocatalysts on both W_2C-modified (Pt/W_2C-C) and WC-modified (Pt/WC-C) mesoporous carbons exhibit a slightly better performance for the ORR than on an unmodified mesoporous support. The corresponding onset potentials of Pt/W_2C-C and Pt/WC-C for ORR are greater than that of the electrocatalyst system prepared with an unmodified mesoporous carbon support (Pt/C). Furthermore, it is clear from Fig. 5 that the reduction currents of Pt/W_2C-C and Pt/WC-C are enhanced in comparison with that of Pt/C. The current increase of Pt/WC-C relative to that of Pt/C is about 170 μA at 0.52 V, indicating a considerable increase in the catalytic activity for the ORR.

In order to determine the number of electron transfers for ORR under experimental conditions, the effect of rotational speeds on currents was investigated at rotation rates ranging from 200 to 2000 rpm. Koutecky–Levich plots were obtained at the potential range between 0.480 and 0.560 V versus SHE. According to the

Table 1
Textural properties of mesoporous carbon supports.

Material	BET surface area ($m^2\ g^{-1}$)	Total pore volume ($cm^3\ g^{-1}$)	Micropore volume ($cm^3\ g^{-1}$)	Pore size (nm)
C-ORNL-1	610	0.63	0.16	7.3
C-$H_3PW_{12}O_{40}$	437	0.44	0.11	6.8
W-C	483	0.52	0.13	6.9
W_2C-C	518	0.54	0.13	6.9
WC-C	384	0.48	0.07	6.9

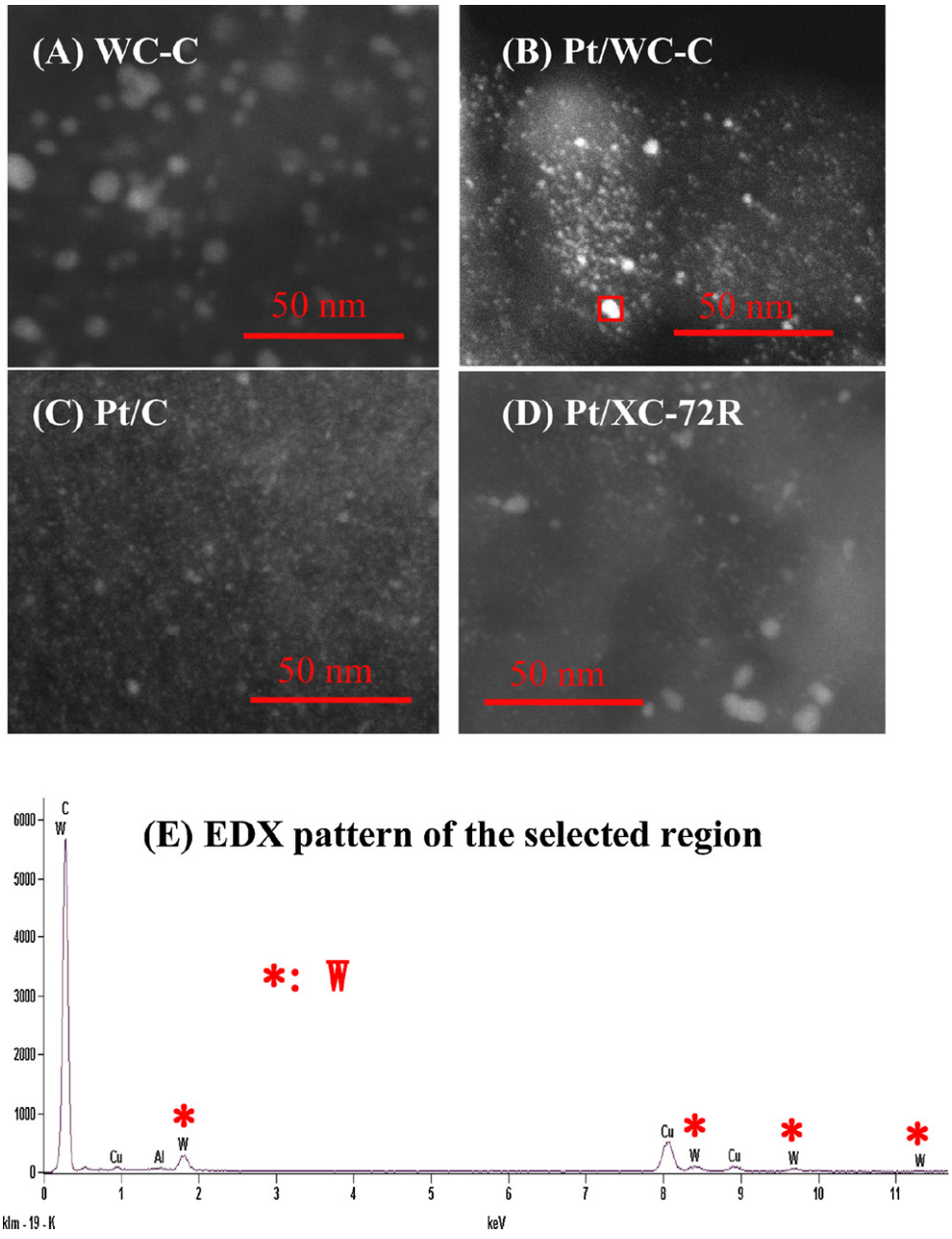

Fig. 4. Dark-field TEM images of WC-C (A), Pt/WC-C (B), Pt/C (C), and Pt/XC-72R (D), and EDX pattern (E) of the selected region from (B).

Koutecky–Levich equation, the following relationship exists:

$$i^{-1} = i_k^{-1} + i_l^{-1} = \frac{1}{nFk\Gamma C_0} + \frac{1}{0.620nFAD_{O_2}^{2/3}\omega^{1/2}\upsilon^{-1/6}C_0}$$

$$= \frac{1}{nFk\Gamma C_0} + \frac{1}{B\omega^{1/2}}$$

where B is $0.620nFAD_{O_2}^{2/3}\upsilon^{-1/6}C_0$; i is the total current; i_k is the kinetic current; i_l is the diffusion-limited current; n is the number of electrons exchanged per mole of O_2; F is the Faraday constant ($96{,}500\ C\ mol^{-1}$); Γ is the quantity of catalyst on the surface of the electrode ($mol\ cm^{-2}$); C_0 is bulk concentration of O_2 in H_2SO_4 solution ($1.03 \times 10^{-6}\ mol\ cm^{-3}$); k is the rate constant for oxygen reduction; A is electrode area (cm^{-2}); D_{O_2} is the diffusion coefficient of O_2 in H_2SO_4 solution ($1.4 \times 10^{-5}\ cm^2\ s^{-1}$); ω is the rotation rate ($rad\ s^{-1}$) and υ is the kinetic viscosity of the water ($0.0107\ cm^2\ s^{-1}$) [28]. The slope of the plot of reciprocal current ($1/I$) versus the reciprocal square root of rotation rate ($1/\omega^{1/2}$) gives B values. The

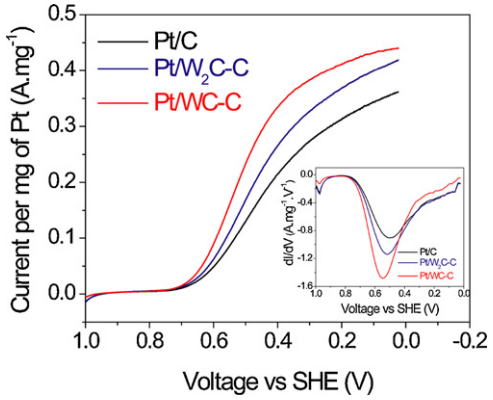

Fig. 5. Linear sweep curves of ORR on different catalysts with Pt loading of ~9 wt%. ORRs were carried out in 0.05 M oxygen-saturated H_2SO_4, the rotation rate of RDE was 1600 rpm, and the potential scan rate was 10 mV s^{-1}. The inset is a plot of the derivative of current versus voltage.

value of n can be calculated from B by using the known parameters mentioned above. As shown in Fig. 6, linear relationships with constant slopes were observed at each potential. The electron transfer numbers were calculated based on the slopes. For both Pt/C and Pt/WC-C, the electron transfer numbers were ~4, suggesting that the oxygen reduction catalyzed by these electrocatalysts follows a four-electron reduction mechanism.

The thermal stabilities of both supports (Fig. 7A) and Pt-loaded electrocatalysts (Fig. 7B) were characterized by TGA. As seen in Fig. 7, the presence of WC increases the oxidation resistance for both supports and Pt-loaded electrocatalysts. Compared with Pt/C, the midpoint of Pt/WC-C at which 50% reduction in mass occurred shifted 40 °C toward the high-temperature side. Although the thermal stability of WC-C was not as good as that of the commercial carbon XC-72R, the Pt/WC-C exhibited higher stability than that of Pt/XC-72R. This result suggested that the synergetic effect between WC and Pt not only enhanced electrochemical activity but also protected the carbon support from oxidation catalyzed by Pt.

To compare the electrochemical stability of Pt/WC-C and Pt/XC-72R, 1000 cycles of CV runs were first performed in the potential range of 0–1.0 V (vs. SHE). Subsequently, linear sweep voltammograms were recorded before and after CV cycles. The potential shift before and after CV cycles can be used to probe the extent of degradation of catalytic activities caused by extended CV cycles. As shown in Fig. 8, although Pt/XC-72R and Pt/WC-C exhibited comparable initial electrochemical activities, after 1000 CV cycles, Pt/WC-C exhibited an obviously smaller shift in potential. When the current was 4×10^{-4} A, a 50 mV potential shift was observed for Pt/WC-C. In contrast, a potential shift of ~85 mV toward the negative side was observed for Pt/XC-72R under similar conditions, suggesting that Pt/WC-C possesses a greater electrochemical stability. The study also found that the electrochemical activity was strongly affected by particle size of the carbon support. The slightly lower electrochemical activity of Pt/WC-C shown in Fig. 8 was attributed to the larger particle size of the Pt/WC-C catalyst. Based on SEM image, the typical particle size of mesoporous carbon support was 1–10 μm, 2–3 order of magnitude greater than commercial carbon (typical particle size of 10–30 nm [29]), resulting in a nonuniform

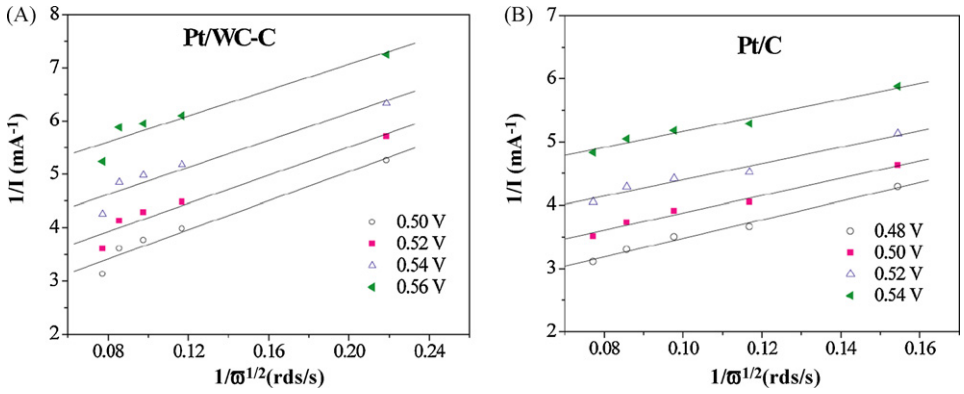

Fig. 6. The relationship between $1/I$ and $1/\omega^{1/2}$ for Pt/WC-C (A) and Pt/C (B).

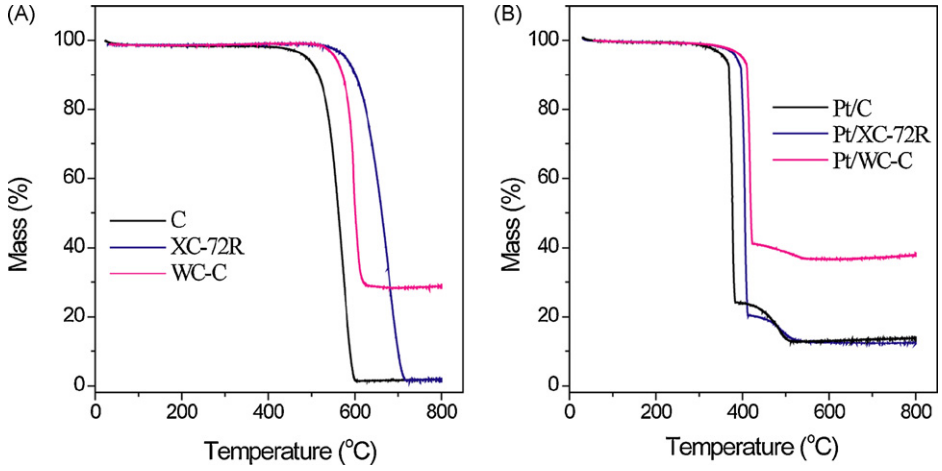

Fig. 7. TGA curves of carbon supports (A) and electrocatalysts (B).

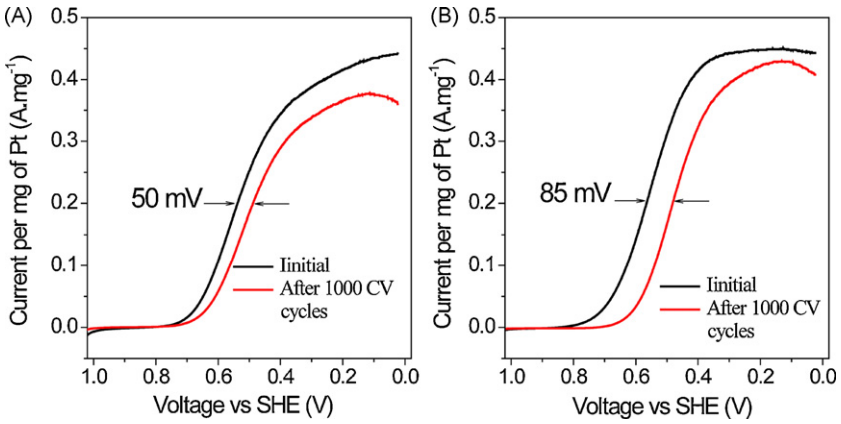

Fig. 8. Electrochemical stability of Pt/WC-C (A) and Pt/XC-72R (B). Loading of Pt was ~9% for both cases. Before and after 1000 CV cycles which were run in a potential window of 0–1.0 V versus SHE at the scan rate of 5 mV s^{-1}, linear sweep voltammogram was recorded to get the potential shift. Oxygen reduction reaction was carried in 0.05 M oxygen-saturated H_2SO_4, RDE rotating rate was 1600 rpm and potential scan rate was 10 mV s^{-1}.

cast of catalyst on RDE and consequently leading to low current density.

4. Conclusions

Both tungsten and tungsten carbide nanoparticles were successfully deposited on mesoporous carbon supports with a high dispersion through a carbothermal reaction of chemisorbed $[PW_{12}O_{40}]^{3-}$ anions with carbon supports under reduction environments and high-temperature treatments. By employing different thermal H_2 reduction treatment temperatures, the mesoporous carbon supports modified by W, W_2C, and WC can be prepared. An ultrahigh Pt dispersion of Pt nanoparticles can be introduced on these surface-modified carbon supports via wet impregnation. We speculate that the high stability of Pt nanoparticles on the mesoporous carbons modified by carbides may be attributed to the enhanced metal–support interaction. Furthermore, an enhancement of the electrochemical activity of Pt for ORR was observed on the carbide-modified supports (WC-C). This increased electrocatalytic activity can be attributed to the synergetic effect between Pt and WC. Our TGA study indicates that the carbide-modified carbon supports are considerably more stable against oxidation than the unmodified carbon support. Both increased high thermal stability and enhanced electrochemical stability exhibited by Pt/WC-C suggest that tungsten carbide-modified mesoporous carbons can be a potential substitute for carbon blacks as an efficient electrocatalyst support.

Acknowledgements

This research was conducted at the Oak Ridge National Laboratory and supported by the U.S. DOE Office of Energy Efficiency and renewable Energy (EERE), under Contract DE-AC05-00OR22725 with Oak Ridge National Laboratory, managed by UT-Battelle, LLC.

References

[1] Y.Y. Shao, G.P. Yin, Y.Z. Gao, J. Power Sources 171 (2007) 558–566.
[2] S.D. Knights, K.M. Colbow, J. St-Pierre, D.P. Wilkinson, J. Power Sources 127 (2004) 127–134.
[3] K.H. Kangasniemi, D.A. Condit, T.D. Jarvi, J. Electrochem. Soc. 151 (2004) E125–E132.
[4] H. Meng, P.K. Shen, Chem. Commun. (2005) 4408–4410.
[5] L.M. Roen, C.H. Paik, T.D. Jarvic, Electrochem. Solid State Lett. 7 (2004) A19–A22.
[6] Y.H. Liu, B.L. Yi, Z.G. Shao, D.M. Xing, H.M. Zhang, Electrochem. Solid State Lett. 9 (2006) A356–A359.
[7] Y.Y. Shao, R. Kou, J. Wang, V.V. Viswanathan, J.H. Kwak, J. Liu, Y. Wang, Y.H. Lin, J. Power Sources 185 (2008) 280–286.
[8] F.B. Su, J.H. Zeng, X.Y. Bao, Y.S. Yu, J.Y. Lee, X.S. Zhao, Chem. Mater. 17 (2005) 3960–3967.
[9] S.H. Joo, S.J. Choi, I. Oh, J. Kwak, Z. Liu, O. Terasaki, R. Ryoo, Nature 412 (2001) 169–172.
[10] C.D. Liang, S. Dai, J. Am. Chem. Soc. 128 (2006) 5316–5317.
[11] P.V. Shanahan, L.B. Xu, C.D. Liang, M. Waje, S. Dai, Y.S. Yan, J. Power Sources 185 (2008) 423–427.
[12] R.B. Levy, M. Boudart, Science 181 (1973) 547–549.
[13] H.H. Hwu, J.G. Chen, J. Phys. Chem. B 107 (2003) 2029–2039.
[14] H. Meng, P.K. Shen, Electrochem. Commun. 8 (2006) 588–594.
[15] H. Meng, P.K. Shen, J. Phys. Chem. B 109 (2005) 22705–22709.
[16] J.A. Nelson, M. Wagner, J. Chem. Mater. 14 (2002) 1639–1642.
[17] J.M. Giraudon, P. Devassine, J.F. Lamonier, L. Delannoy, L. Leclercq, G. Leclercq, J. Solid State Chem. 154 (2000) 412–426.
[18] L. Volpe, M. Boudart, J. Solid State Chem. 59 (1985) 348–356.
[19] C.H. Liang, F.P. Tian, Z.L. Li, Z.C. Feng, Z.B. Wei, C. Li, Chem. Mater. 15 (2003) 4846–4853.
[20] C. Moreno-Castilla, M.A. Alvarez-Merino, F. Carrasco-Marin, J.L.G. Fierro, Langmuir 17 (2001) 1752–1756.
[21] X.Q. Wang, C.D. Liang, S. Dai, Langmuir 24 (2008) 7500–7505.
[22] I.V. Kozhevnikov, A. Sinnema, R.J.J. Jansen, H. Vanbekkum, Catal. Lett. 27 (1994) 187–197.
[23] N. Mizuno, M. Misono, Chem. Rev. 98 (1998) 199–217.
[24] M. Sadakane, E. Steckhan, Chem. Rev. 98 (1998) 219–237.
[25] S.J. Dong, Z. Jin, J. Chem. Soc., Chem. Commun. (1987) 1871–1872.
[26] D. Martel, N. Sojic, A. Kuhn, J. Chem. Educ. 79 (2002) 349–352.
[27] M. Zhou, L.P. Guo, F.Y. Lin, H.X. Liu, Anal. Chim. Acta 587 (2007) 124–131.
[28] O. Solorza-Feria, S. Citalan-Cigarroa, R. Rivera-Noriega, S.M. Fernandez-Valverde, Electrochem. Commun. 1 (1999) 585–589.
[29] M. Gustavsson, H. Ekstrom, R. Hanarp, L. Eurenius, G. Lindbergh, E. Olsson, B. Kasemo, J. Power Sources 163 (2007) 671–678.